Supplemental Information

Force-mediated molecule release from double network hydrogels

Pavithra B Jayathilaka, [a] Thomas G Molley, [b] Yuwan Huang,[c] M. Shariful Islam, [b] Michael Robert Buche, [d] Meredith Silberstein, [d] Jamie J. Kruzic, [c] Kristopher A. Kilian,[a,b*]

[a] School of Chemistry, University of New South Wales (UNSW Sydney), Sydney NSW 2052, Australia
[b] School of Materials Science, University of New South Wales (UNSW Sydney), Sydney NSW 2052, Australia
[c] Sibley School of Mechanical and Aerospace Engineering, Cornell University, Ithaca, NY, USA

Materials

All commercially available materials were obtained from Sigma-Aldrich and were used as they were received without further purification unless otherwise specified. $CaCl_2$, Acetylene dicarboxylate, toluene, Diethyl ether (Et_2O), $NaHCO_3$, NaCl, $MgSO_4$, Celite, Ethyl acetate, hexanes, ethanol, and DMSO were purchased from CAS Scientific's ChemSupply. Silica gel was purchased from Silicycle Inc. All chemicals were reagent grade or better.

Instrumentation and Analysis

NMR characterization

Synthesized samples were dissolved in $CDCl_3$ at a final concentration of 10 mg/ml and transferred to an NMR sample tube. ^{1}H NMR spectra were recorded on Bruker BioSpin 400.13 MHz spectrometer at 293 K with 8 scans and a delay of 5 s. Chemical shifts were reported in delta (δ) units and expressed in parts per million (ppm) downfield from tetramethylsilane (TMS) using $CDCl_3$, 1H: 0.0 ppm as an internal standard. ^{1}H NMR data was first phased, and baseline corrected (Bernstein polynomial fit, order 3) using MNOVa software (MestRelab Research S.L version: 14.0.0-23239).

FTIR characterization

Fourier Transform Infrared (FTIR) spectrometer with attenuated total reflectance (ATR) was used to characterize gel samples, and spectra were recorded on Spectrum software. Hydrogels and organic samples (opaque oils, solids, and powders ranging from 22 µm to 2.5 µm) were analysed from 450-4000 cm^{-1} wavelength range.

Raman spectroscopy

Gels were dried at room temperature for overnight to remove the water before Raman studies. All measurements were carried out at room temperature. Raman spectra were collected by Renishaw (inVia 2) Raman spectrometer coupled to a microscope (Leica.), and spectra were recorded on Wire 5.3 software. The microscope focused a diode laser (785 nm, 9.6 mW, with1200 l / mm grating) onto the sample (~0.8 µm spot size) on exciting through a 5x magnification lens (Leica) and collected the light scattered off the sample surface. The scattered light was directed through the Raman spectrometer to obtain spectral data. Spectra were recorded from 600 cm^{-1} to 1800 cm^{-1}.

Experimental Procedures:

Synthesis

Step 1:

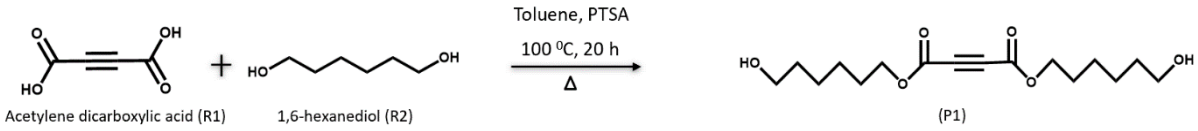

Figure S1: Mechanophore synthesis reaction step 1

Synthesis protocols are based on the literature which were modified during the experiments.[63] Esterification reaction was performed with mixing acetylene dicarboxylate (5.0 g, 43.8 mmol), 1,6-hexanediol (52 g, 438 mmol) in 70 ml of toluene. The catalyst, p-toluenesulfonic acid monohydrate (PTSA) (833 mg, 4.38 mmol), was added to the mixture. The reaction proceeded for 20 h at 100 °C. The generated water during the reaction was collected using a Dean-Stark trap, which was fitted to the reflux condenser. After 20 h, around ca.1.2 ml of water was collected, and the setup was allowed to reach room temperature. The solution was diluted with Et_2O (50 mL) and cooled at -10 °C for 1 hour. Then the solution was decanted, and the precipitate was washed with an excess of Et_2O. The combined organic solution was washed with saturated $NaHCO_3$ solution (2 × 50 mL), water (4 × 50 mL), and brine (1 × 50 mL), respectively. The resultant organic layer was dried with Mg_2SO_4, followed by filtering through a Celite pad. The product was concentrated under a vacuum to evaporate solvents. The resultant product was a pale-yellow oil with a yield of 46%. 1H NMR (400 MHz, $CDCl_3$) δ 4.20 (t, 4H), 3.61 (t, 4H), 1.70 – 1.60 (m, 4H), 1.55(m, 4H), 1.40 – 1.30(m, 8H).

Step 2:

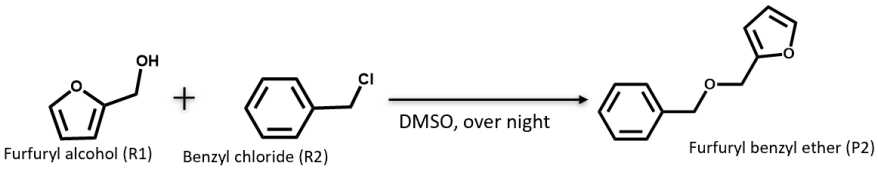

Figure S2: Mechanophore synthesis reaction step 2

Furfuryl alcohol was stirred in DMSO at room temperature overnight. After 1 h, benzyl chloride was added into the reaction mixture. The reaction was monitored via thin-layer chromatography (TLC). The crude product was purified with a silica column, and the yield was pale yellow liquid (98%).[64] 1H NMR (400 MHz, CDCl3) δ = 7.40–7.06 (m, 6H,), 6.26 (d, J = 4.0 Hz), 4.47 (s, 2H), 4.41 (s, 2H,)

Step 3:

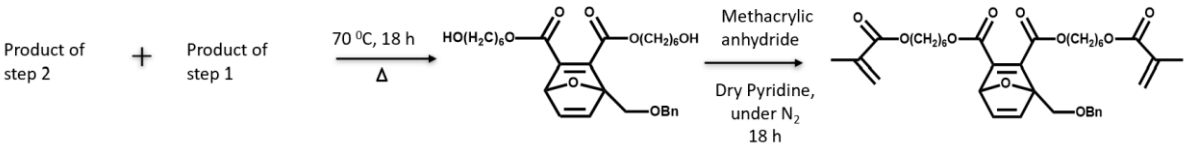

Figure S3: Mechanophore synthesis reaction step 3

Product of step 1 reaction (P1) (3.5 g, 11.1 mmol) and the product from step 2 (P2) of 2.31 g, 12.2 mmol, were reacted at 70 °C for 20 hours in a sealed vial. The reaction was monitored via ^{1}H NMR spectroscopy. When the reaction was completed, the mixture was allowed to come to room temperature. Then the excess unreacted starting materials were removed by triturating with hexane ((3 × 15 mL). Excess solvent was removed under vacuum, and the intermediate diol yield was dark orange oil (70%)

The intermediate diol was reacted with (298 mg, 0.59 mmol) methacrylic anhydride (660 µL, 4.4 mmol) in dry pyridine under an N_2 environment for 18 h. The reaction was monitored with TLC (85% EtOAc/hexanes). The mixture was diluted with Et2O (10 mL) and successively washed with water (2 × 10 mL) and 10 wt% $CuSO_4$ solutions (3 × 10 mL) followed by saturated $NaHCO_3$ solution (2 × 10 mL). The resultant organic layer was dried with Mg_2SO_4 and vacuumed to get the crude product. The crude product was purified with flash column chromatography (20% EtOAc/hexanes) (R_f = 0.85). The yield was pale yellow oil (9.5%). 1H NMR (400 MHz,

$CDCl_3$) δ 7.40 – 7.29 (m, 5H), 7.20 (s, 1H), 6.99 (d, *J* = 5.2 Hz, 1H), 6.09 (s, 2H), 5.70 (s, 1H), 5.55 (s, 2H), , 462 (s,2H), 4.55 (s,2H), 4.23 – 4.07 (m, 8H), 1.94 (s, 6H), 1.70 – 1.62 (m, 8H), 1.45 – 1.35 (m, 8H).

Step 1 product (P1) –

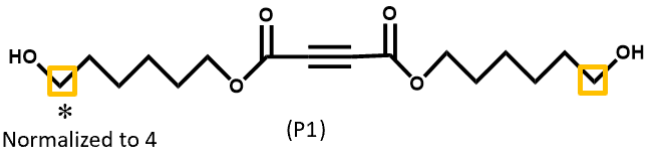

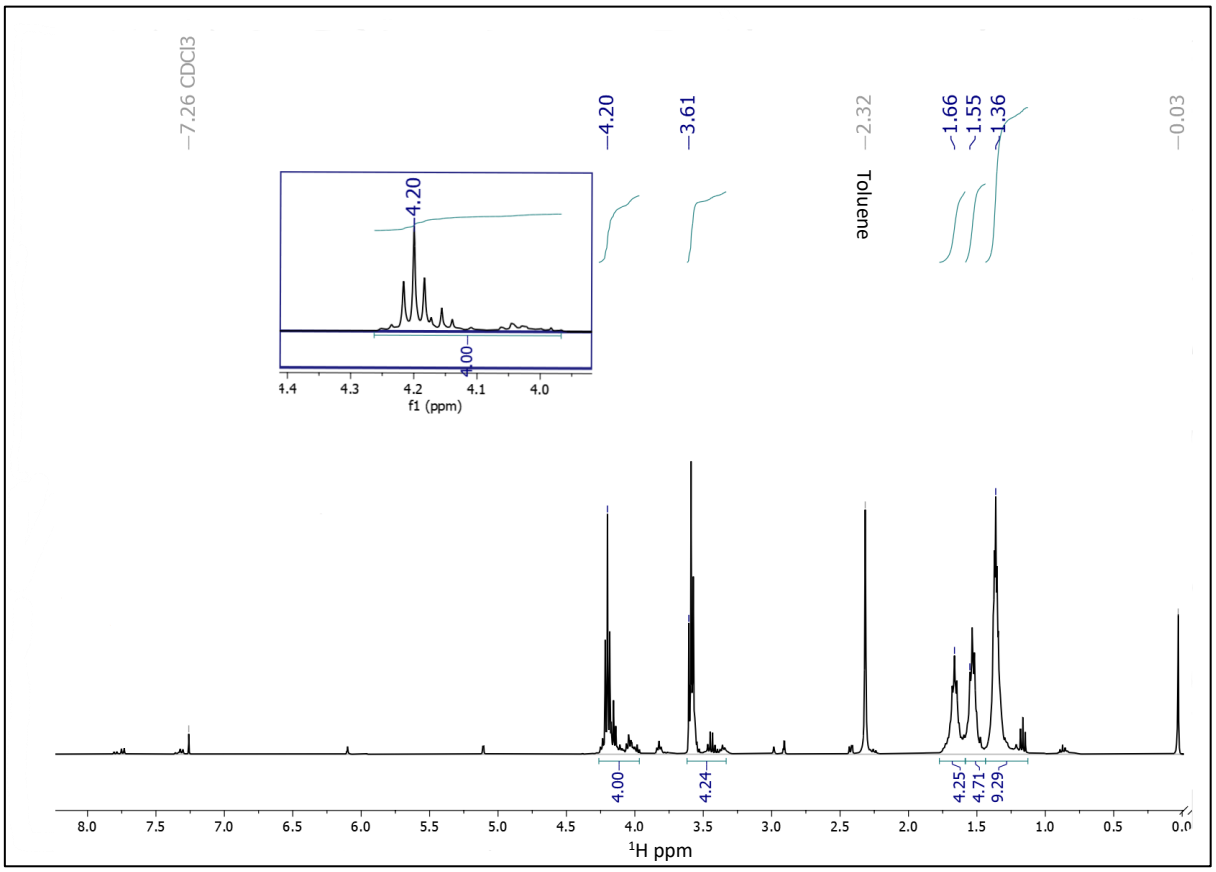

Figure S4: ^{1}H NMR spectrum of P1. Inset: magnified 4.4– 4.0 ppm region

Step 2 product (P2) :

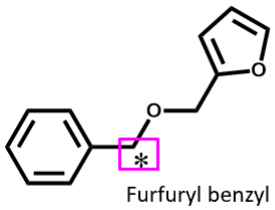

Furfuryl benzyl ether (P2)

Normalized to 2

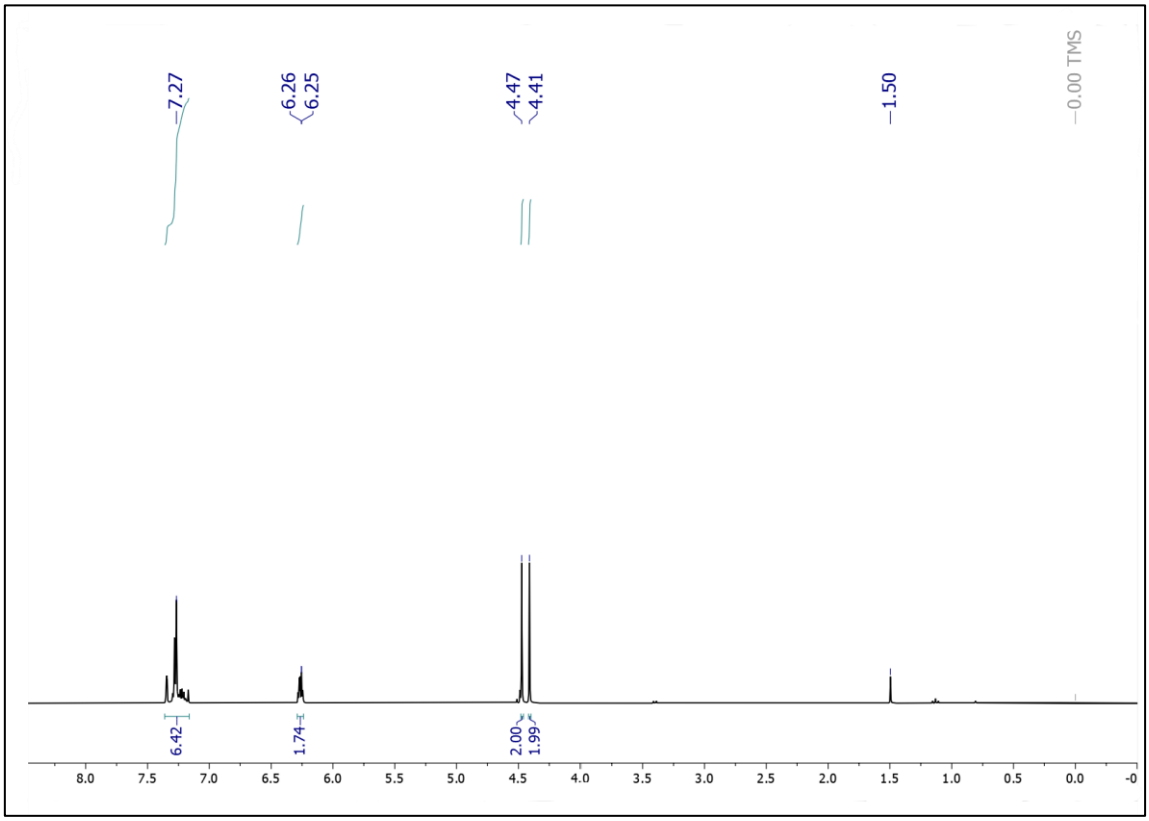

Figure S5: ^{1}H NMR spectrum of P2

Step 3 mechanophore –

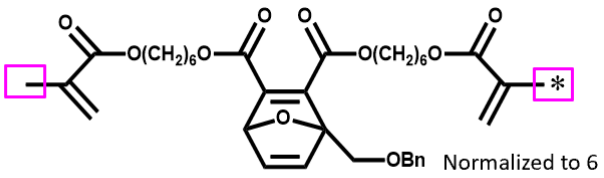

Figure S6: ^{1}H NMR spectrum of mechanophore

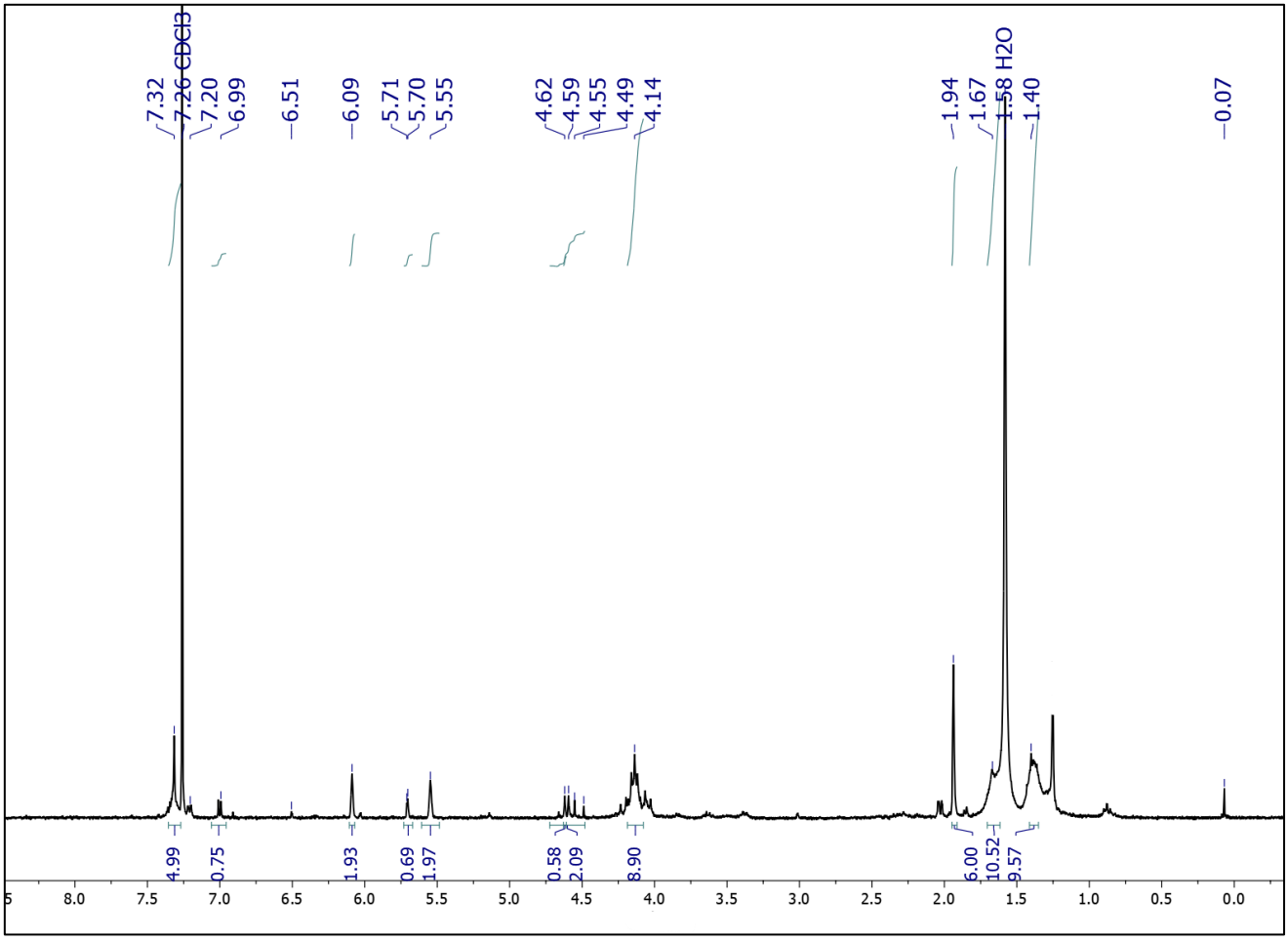

Preparation of double network hydrogels

5 wt% oxanorbornadiene mechanophore in DMSO was dissolved in 95 wt% acrylamide containing 1.45 wt% alginate with a final volume of 1 mL. Ammonium persulphate (5.0 µL) as a photo-initiator and N,N,N',N'-tetramethylethylenediamine (TEMED) (0.5 µL) as the crosslinking accelerator were added to the mixture. The solution was poured into a glass mold for the covalent network to polymerize. After 45 min of gelation time, the hydrogel was washed with water to remove DMSO with DMSO removal monitored with FTIR. After complete removal of DMSO the sample was immersed in 3 wt% $CaCl_2$ solution overnight and stored until use.

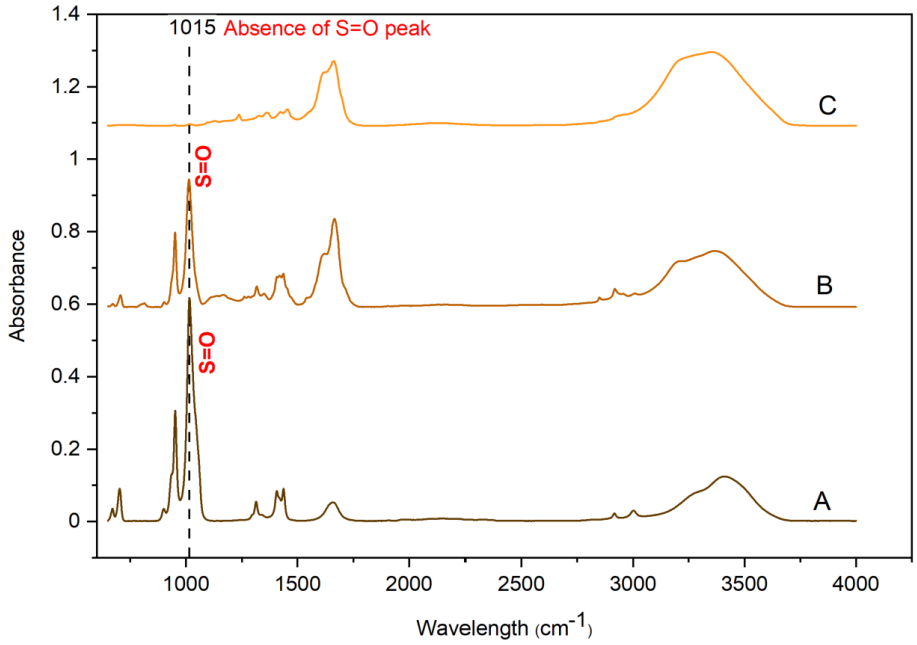

Figure S7: Evaluation of DMSO removal by FTIR. a) FTIR spectrum of DMSO, which shows characteristic S=O bond peak at 1015 cm $^{-1}$. b) FTIR spectrum of the hydrogel before removing DMSO. c) FTIR spectrum of the hydrogel before removing DMSO, which confirms the removal of DMSO by the absence of S=O peak at 1015 cm^{-1}.

Mechanical tests

Specimens were removed from the $CaCl_2$ storage solution, excess fluid removed with shaking and wicking with a Kim wipe, and immediately subjected to compression in a humid environment. The compression tests were performed by a universal testing instrument (ElectroPuls E1000, Instron) with a 250 N load cell (Instron). The test speed was 1 mm/min, and the load was held on the sample for 5 min. Engineering stress-strain curves were presented after tests. The strain and stress were calculated using the two equation $\varepsilon_e = \frac{\Delta h}{h_o}$ and $\sigma_e = \frac{F}{A_0}$, where h_0 and A_0 are the original height and cross-sectional area of the uncompressed sample, Δh is the change in height, *F*

is the applied force. The compressive modulus was defined as the ratio of stress to strain in the initial compression region and determined using the average slope of fitting line within 5-10% strain range.

Mechanical test was performed on cubic samples following table shows each dimension.

TABLE 1 Sample dimensions

Compression stress	*Dimensions (mm)*
0.01 MPa	*6.20 × 5.60 × 5.40*
0.05 MPa	*5.80 × 5.60 × 5.90*
0.10 MPa	*5.70 × 5.00 × 4.90*
0.05 MPa	*4.80 × 5.00 × 4.50*
1.00 MPa	*5.00 × 4.50 × 5.40*
2.00 MPa	*4.50 × 4.20 × 5.20*

GC-MS analysis

Molecule release under compression was monitored with gas chromatography-mass spectrometry (GC-MS). GC analysis were carried out using a Shimadzu GCMS QP2010Plus with diphenyl/methyl column (30m × 0.32mm × 0.25 µm film thickness on GC system with a flame ionization detector (FID)

Data analysis

All Raman, FTIR, and GC-MS acquired data were analyzed by Origin2020b software. Origin2020b software was used for the statistical analysis to show differences between groups (One-way ANOVA). Significant difference is indicated when $P < 0.05$.

The percentage of molecule was calculated as

$$Release\ \% = \frac{amount\ of\ molecule\ release\ (g) \times 100}{amount\ of\ molecules\ loaded\ on\ gel(g)}$$

TABLE 2 Assignment of Raman bands

Reported (cm $^{-1}$)[65-67]	Observed in this work		Assignment
	PAAm	Oxo	
641	641	644	τ, CH_2
667 [66]		677	Norbornadiene ω, CH
780	779	775	ω, CH
844	842	844	Γ, CH2
800-970 [68]		951	υ, (C-O-C)
1000 [68]		1005	υ, (CC) aromatic ring
1113	1107	1111	υ, (C-C)
1209	1212	1220	ω, NH_2
1326	1324	1328	δ, CH
1430	1429	1422	υ, C-N
1457	1452	1456	δ, CH_2
1516		1516	Norbornadiene C=C
1607	1608	1616	δ, NH_2
1665	1669	1664	υ, C=O in amide

v_a and v_s - asymmetric and symmetric stretching, δ - bending, ω - wagging, Γ - twisting, τ - torsion

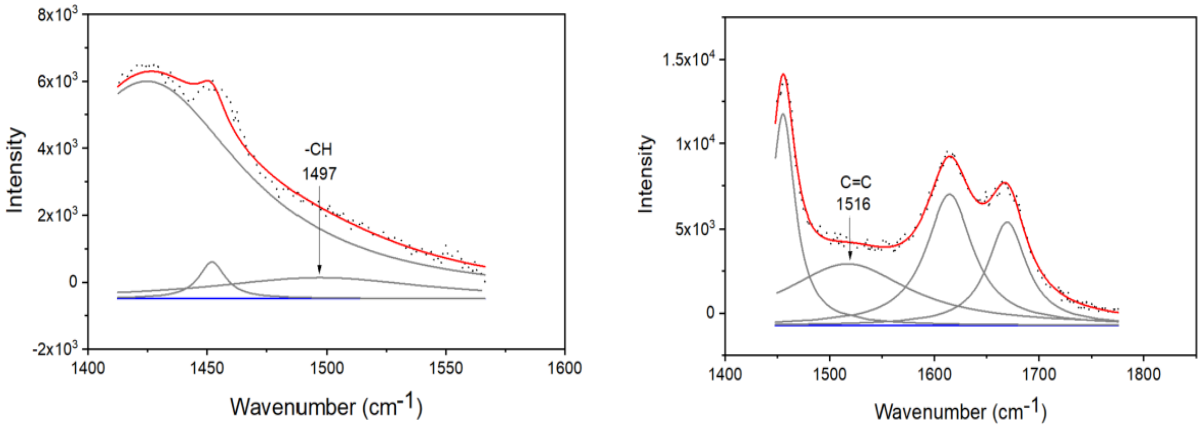

Figure S8: Curve fitting Raman spectra with deconvolution into the Lorentz components after baseline subtraction a) Acrylamide gel (control) b) mechanophore-linked hydrogel, which shows the presence of C=C bond of oxanorbornadiene mechanophore

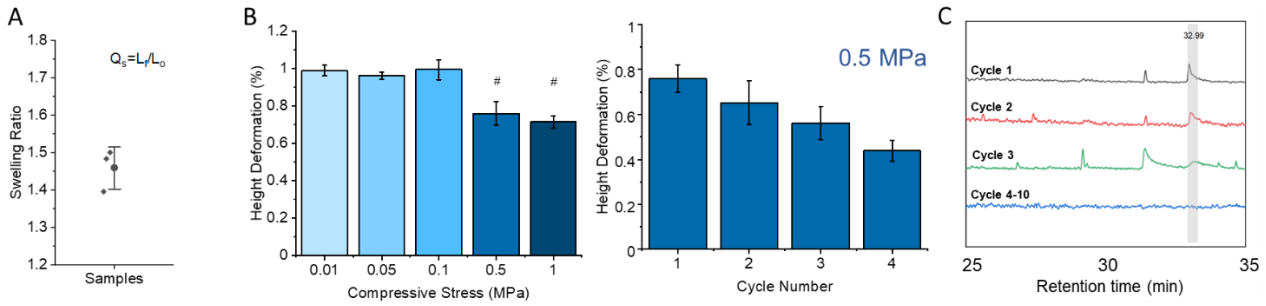

Figure S9. (a) Swelling analysis for mechanophore crosslinked double network hydrogels. (b) change in specimen geometry after compression at different forces (left) and during cyclic loading at 0.5 MPa (right). (c) GC elution analysis of samples compressed in the same direction up to ten times. #signifies p<0.005 compared to 0.01, 0.05 and 0.1 MPa compression.

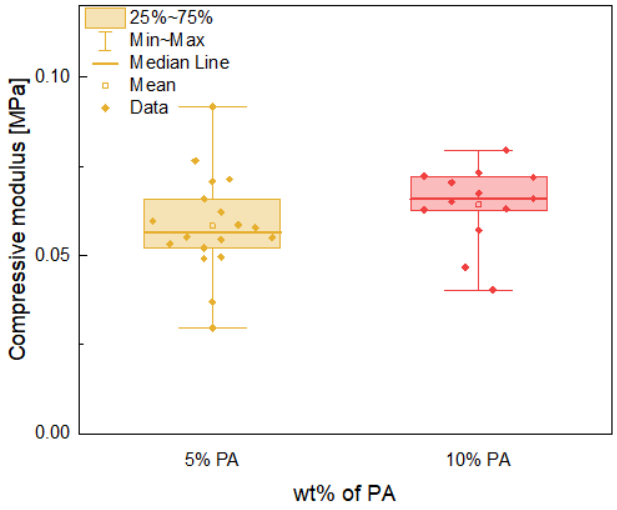

Figure S10: Box and whisker plots of the compressive modulus of 5% and 10% mechanophore containing samples based on 18 repeat experiments for the 5% case and 13 repeat experiments for the 10% case.

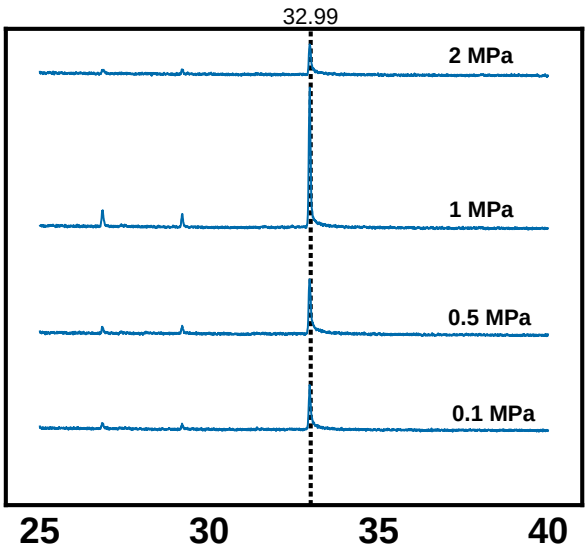

Figure S11: GC-MS trace showing elution of the Oxo-OBn molecular release.

Theoretical modelling of molecule release

The model for small molecule release in the double network hydrogel was adapted from [62] to include an irreversible reaction (molecule release) that does not result in fracture of the polymer chains, in addition to a later irreversible scission of the chains. In brief, this model starts from the statistical mechanical description of a single polymer chain and predicts the stress response and mechanochemical response of the polymer network when subjected to mechanical deformation. The parameters in this model are the number of links in a single chain segment, N_b; the volumetric swelling ratio, J; the total number density of chains, n; the nondimensional link stiffness, κ; the nondimensional end-to-end length of the chain that triggers the release, $\gamma_{release}$; and the nondimensional end-to-end length that results in scission of the chain, $\gamma_{scission.}$ The values for these parameters are given in Table 2. The first three parameters were directly determined by the polymer chemistry: N_b was determined by the average number of monomers between crosslinks; J was estimated from the water content compared to the dry polymer content; and nkT was determined such that the model matched the median elastic modulus from the experiments of 56 kPa. κ and $\gamma_{scission}$ were calibrated to the mechanical response of the material, while $\gamma_{release}$ was then calibrated to the corresponding release percentage. [62] The model is stiffer than the experimental data at large strain primarily because we neglect the increase in contour length that results from the small molecule release.

TABLE 2. Parameters for double network hydrogel model

Parameter	Value
N_b	85
J	10
nkT	36.56 kPa
κ	2000
$\gamma_{release}$	0.575
$\gamma_{scission}$	1

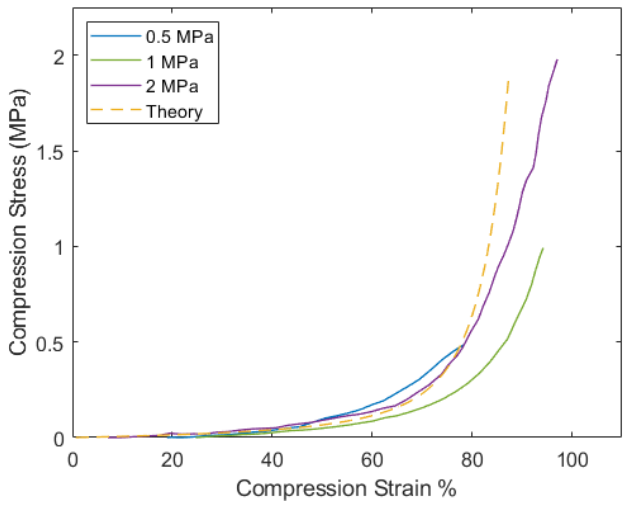

Figure S12: Engineering stress-strain plots of experimental data for the 5% gel compression alongside the theoretical model

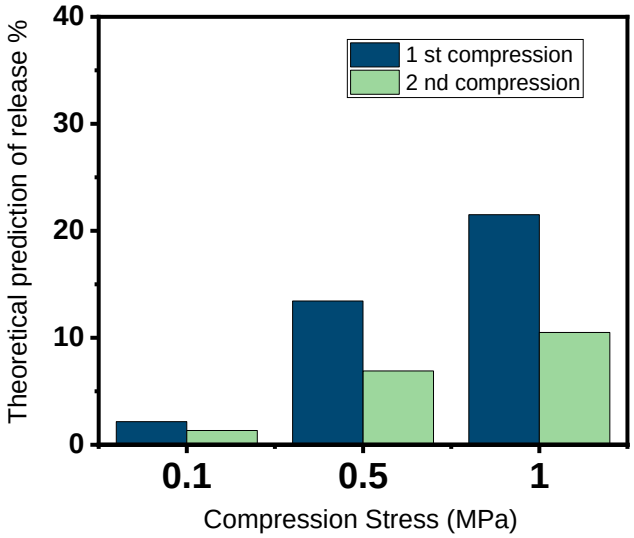

Figure S13. Theoretical molecule release predicted after the first compression and the second compression with 90° rotation.

References

1. Larsen, M. B.; Boydston, A. J., Investigations in fundamental and applied polymer mechanochemistry. *Macromolecular Chemistry and Physics* **2016,** *217* (3), 354-364.
2. Costa, A. M.; Mano, J. F., Extremely strong and tough hydrogels as prospective candidates for tissue repair–A review. *European Polymer Journal* **2015,** *72*, 344-364.
3. Li, J.; Nagamani, C.; Moore, J. S., Polymer mechanochemistry: from destructive to productive. *Accounts of chemical research* **2015,** *48* (8), 2181-2190.
4. Facchi, D. P.; Cazetta, A. L.; Canesin, E. A.; Almeida, V. C.; Bonafé, E. G.; Kipper, M. J.; Martins, A. F., New magnetic chitosan/alginate/Fe3O4@ SiO2 hydrogel composites applied for removal of Pb (II) ions from aqueous systems. *Chemical Engineering Journal* **2018,** *337*, 595-608.
5. Abi Ghanem, M.; Basu, A.; Behrou, R.; Boechler, N.; Boydston, A. J.; Craig, S. L.; Lin, Y.; Lynde, B. E.; Nelson, A.; Shen, H., The role of polymer mechanochemistry in responsive materials and additive manufacturing. *Nature Reviews Materials* **2020**, 1-15.
6. Staudinger, H.; Bondy, H., Isoprene and rubber. XIX. The molecular size of rubber and balata. *Rubber Chemistry and Technology* **1930,** *3* (3), 519-521.
7. Black, A. L.; Lenhardt, J. M.; Craig, S. L., From molecular mechanochemistry to stress-responsive materials. *Journal of Materials Chemistry* **2011,** *21* (6), 1655-1663.
8. Sottos, N. R., Polymer mechanochemistry: Flex, release and repeat. *Nature chemistry* **2014,** *6* (5), 381.
9. Brantley, J. N.; Wiggins, K. M.; Bielawski, C. W., Polymer mechanochemistry: the design and study of mechanophores. *Polymer international* **2013,** *62* (1), 2-12.
10. May, P. A.; Moore, J. S., Polymer mechanochemistry: techniques to generate molecular force via elongational flows. *Chemical Society Reviews* **2013,** *42* (18), 7497-7506.
11. Beiermann, B. A.; Kramer, S. L.; Moore, J. S.; White, S. R.; Sottos, N. R., Role of mechanophore orientation in mechanochemical reactions. *Acs Macro Letters* **2012,** *1* (1), 163-166.
12. Beiermann, B. A.; Davis, D. A.; Kramer, S. L.; Moore, J. S.; Sottos, N. R.; White, S. R., Environmental effects on mechanochemical activation of spiropyran in linear PMMA. *Journal of Materials Chemistry* **2011,** *21* (23), 8443-8447.
13. Beiermann, B. A.; Kramer, S. L.; May, P. A.; Moore, J. S.; White, S. R.; Sottos, N. R., The effect of polymer chain alignment and relaxation on force-induced chemical reactions in an elastomer. *Advanced Functional Materials* **2014,** *24* (11), 1529-1537.

14. Chen, Y.; Mellot, G.; van Luijk, D.; Creton, C.; Sijbesma, R. P., Mechanochemical tools for polymer materials. *Chemical Society Reviews* **2021**.
15. Davis, D. A.; Hamilton, A.; Yang, J.; Cremar, L. D.; Van Gough, D.; Potisek, S. L.; Ong, M. T.; Braun, P. V.; Martínez, T. J.; White, S. R., Force-induced activation of covalent bonds in mechanoresponsive polymeric materials. *Nature* **2009,** *459* (7243), 68-72.
16. Degen, C. M.; May, P. A.; Moore, J. S.; White, S. R.; Sottos, N. R., Time-dependent mechanochemical response of SP-cross-linked PMMA. *Macromolecules* **2013,** *46* (22), 8917-8921.
17. Lee, C. K.; Beiermann, B. A.; Silberstein, M. N.; Wang, J.; Moore, J. S.; Sottos, N. R.; Braun, P. V., Exploiting force sensitive spiropyrans as molecular level probes. *Macromolecules* **2013,** *46* (10), 3746-3752.
18. Li, M.; Zhang, Q.; Zhou, Y.-N.; Zhu, S., Let spiropyran help polymers feel force! *Progress in Polymer Science* **2018,** *79*, 26-39.
19. Chen, Y.; Spiering, A.; Karthikeyan, S.; Peters, G. W.; Meijer, E.; Sijbesma, R. P., Mechanically induced chemiluminescence from polymers incorporating a 1, 2-dioxetane unit in the main chain. *Nature chemistry* **2012,** *4* (7), 559.
20. Robb, M. J.; Moore, J. S., A retro-staudinger cycloaddition: Mechanochemical cycloelimination of a β-lactam mechanophore. *Journal of the American Chemical Society* **2015,** *137* (34), 10946-10949.
21. Kryger, M. J.; Ong, M. T.; Odom, S. A.; Sottos, N. R.; White, S. R.; Martinez, T. J.; Moore, J. S., Masked cyanoacrylates unveiled by mechanical force. *Journal of the American Chemical Society* **2010,** *132* (13), 4558-4559.
22. Karman, M.; Verde-Sesto, E.; Weder, C.; Simon, Y. C., Mechanochemical Fluorescence Switching in Polymers Containing Dithiomaleimide Moieties. *ACS Macro Letters* **2018,** *7* (9), 1099-1104.
23. Sagara, Y.; Karman, M.; Verde-Sesto, E.; Matsuo, K.; Kim, Y.; Tamaoki, N.; Weder, C., Rotaxanes as mechanochromic fluorescent force transducers in polymers. *Journal of the American Chemical Society* **2018,** *140* (5), 1584-1587.
24. Black, A. L.; Orlicki, J. A.; Craig, S. L., Mechanochemically triggered bond formation in solid-state polymers. *Journal of Materials Chemistry* **2011,** *21* (23), 8460-8465.
25. Diesendruck, C. E.; Steinberg, B. D.; Sugai, N.; Silberstein, M. N.; Sottos, N. R.; White, S. R.; Braun, P. V.; Moore, J. S., Proton-coupled mechanochemical transduction: a mechanogenerated acid. *J Am Chem Soc* **2012,** *134* (30), 12446-9.
26. Xia, T.; Liu, W.; Yang, L., A review of gradient stiffness hydrogels used in tissue engineering and regenerative medicine. *Journal of Biomedical Materials Research Part A* **2017,** *105* (6), 1799-1812.
27. Bowser, B. H.; Craig, S. L., Empowering mechanochemistry with multi-mechanophore polymer architectures. *Polymer Chemistry* **2018,** *9* (26), 3583-3593.
28. Barber, R. W.; McFadden, M. E.; Hu, X.; Robb, M. J., Mechanochemically Gated Photoswitching: Expanding the Scope of Polymer Mechanochromism. *Synlett* **2019,** *30* (15), 1725-1732.
29. Deneke, N.; Rencheck, M. L.; Davis, C. S., An engineer's introduction to mechanophores. *Soft Matter* **2020,** *16* (27), 6230-6252.
30. Wang, J.; Kouznetsova, T. B.; Kean, Z. S.; Fan, L.; Mar, B. D.; Martínez, T. J.; Craig, S. L., A remote stereochemical lever arm effect in polymer mechanochemistry. *Journal of the American Chemical Society* **2014,** *136* (43), 15162-15165.
31. Ghanem, M. A.; Basu, A.; Behrou, R.; Boechler, N.; Boydston, A. J.; Craig, S. L.; Lin, Y.; Lynde, B. E.; Nelson, A.; Shen, H.; Storti, D. W., The role of polymer mechanochemistry in responsive materials and additive manufacturing. *Nature Reviews Materials* **2020,** *6* (1), 84-98.
32. Rohde, R. C.; Basu, A.; Okello, L. B.; Barbee, M. H.; Zhang, Y.; Velev, O. D.; Nelson, A.; Craig, S. L., Mechanochromic composite elastomers for additive manufacturing and low strain mechanophore activation. *Polymer Chemistry* **2019,** *10* (44), 5985-5991.
33. Davis, D. A.; Hamilton, A.; Yang, J.; Cremar, L. D.; Van Gough, D.; Potisek, S. L.; Ong, M. T.; Braun, P. V.; Martinez, T. J.; White, S. R.; Moore, J. S.; Sottos, N. R., Force-induced activation of covalent bonds in mechanoresponsive polymeric materials. *Nature* **2009,** *459* (7243), 68-72.
34. Li, Z. a.; Toivola, R.; Ding, F.; Yang, J.; Lai, P. N.; Howie, T.; Georgeson, G.; Jang, S. H.; Li, X.; Flinn, B. D., Highly sensitive built-in strain sensors for polymer composites: Fluorescence turn-on response through mechanochemical activation. *Advanced Materials* **2016,** *28* (31), 6592-6597.

35. Calvino, C.; Guha, A.; Weder, C.; Schrettl, S., Self-Calibrating Mechanochromic Fluorescent Polymers Based on Encapsulated Excimer-Forming Dyes. *Adv Mater* **2018,** *30* (19), e1704603.
36. Grady, M. E.; Beiermann, B. A.; Moore, J. S.; Sottos, N. R., Shockwave loading of mechanochemically active polymer coatings. *ACS Appl Mater Interfaces* **2014,** *6* (8), 5350-5.
37. Karman, M.; Verde-Sesto, E.; Weder, C.; Simon, Y. C., Mechanochemical Fluorescence Switching in Polymers Containing Dithiomaleimide Moieties. *ACS Macro Letters* **2018**, 1099-1104.
38. Peterson, G. I.; Larsen, M. B.; Ganter, M. A.; Storti, D. W.; Boydston, A. J., 3D-printed mechanochromic materials. *ACS applied materials & interfaces* **2015,** *7* (1), 577-583.
39. Piermattei, A.; Karthikeyan, S.; Sijbesma, R. P., Activating catalysts with mechanical force. *Nature chemistry* **2009,** *1* (2), 133-137.
40. Diesendruck, C. E.; Steinberg, B. D.; Sugai, N.; Silberstein, M. N.; Sottos, N. R.; White, S. R.; Braun, P. V.; Moore, J. S., Proton-coupled mechanochemical transduction: a mechanogenerated acid. *Journal of the American Chemical Society* **2012,** *134* (30), 12446-12449.
41. Gunckel, R.; Koo, B.; Xu, Y.; Pauley, B.; Hall, A.; Chattopadhyay, A.; Dai, L. L., Grafted Cinnamoyl-based Mechanophores for Self-Sensing and Photochemical Healing Capabilities in Epoxy. *ACS Applied Polymer Materials* **2020,** *2* (9), 3916-3928.
42. Gossweiler, G. R.; Hewage, G. B.; Soriano, G.; Wang, Q.; Welshofer, G. W.; Zhao, X.; Craig, S. L., Mechanochemical activation of covalent bonds in polymers with full and repeatable macroscopic shape recovery. *ACS Macro Letters* **2014,** *3* (3), 216-219.
43. Robb, M. J.; Moore, J. S., A Retro-Staudinger Cycloaddition: Mechanochemical Cycloelimination of a beta-Lactam Mechanophore. *J Am Chem Soc* **2015,** *137* (34), 10946-9.
44. Diesendruck, C. E.; Peterson, G. I.; Kulik, H. J.; Kaitz, J. A.; Mar, B. D.; May, P. A.; White, S. R.; Martínez, T. J.; Boydston, A. J.; Moore, J. S., Mechanically triggered heterolytic unzipping of a low-ceiling-temperature polymer. *Nature chemistry* **2014,** *6* (7), 623-628.
45. Larsen, M. B.; Boydston, A. J., Successive mechanochemical activation and small molecule release in an elastomeric material. *Journal of the American Chemical Society* **2014,** *136* (4), 1276-1279.
46. Hu, X.; Zeng, T.; Husic, C. C.; Robb, M. J., Mechanically Triggered Small Molecule Release from a Masked Furfuryl Carbonate. *J Am Chem Soc* **2019,** *141* (38), 15018-15023.
47. Sottos, N. R., Polymer mechanochemistry: Flex, release and repeat. *Nat Chem* **2014,** *6* (5), 381-3.
48. Lavalle, P.; Boulmedais, F.; Schaaf, P.; Jierry, L., Soft-mechanochemistry: mechanochemistry inspired by nature. *Langmuir* **2016,** *32* (29), 7265-7276.
49. Wang, L.; Zhou, W.; Tang, Q.; Yang, H.; Zhou, Q.; Zhang, X., Rhodamine-functionalized mechanochromic and mechanofluorescent hydrogels with enhanced mechanoresponsive sensitivity. *Polymers* **2018,** *10* (9), 994.
50. Ballance, W. C.; Seo, Y.; Baek, K.; Chalifoux, M.; Kim, D.; Kong, H., Stretchable, anti-bacterial hydrogel activated by large mechanical deformation. *J Control Release* **2018,** *275*, 1-11.
51. Chen, H.; Yang, F.; Chen, Q.; Zheng, J., A Novel Design of Multi-Mechanoresponsive and Mechanically Strong Hydrogels. *Adv Mater* **2017,** *29* (21).
52. Chen, J.; Peng, Q.; Peng, X.; Han, L.; Wang, X.; Wang, J.; Zeng, H., Recent advances in mechano-responsive hydrogels for biomedical applications. *ACS Applied Polymer Materials* **2020,** *2* (3), 1092-1107.
53. Matsuda, T.; Kawakami, R.; Namba, R.; Nakajima, T.; Gong, J. P., Mechanoresponsive self-growing hydrogels inspired by muscle training. *Science* **2019,** *363* (6426), 504-508.
54. Mier, L. J.; Adam, G.; Kumar, S.; Stauch, T., The Mechanism of Flex-Activation in Mechanophores Revealed By Quantum Chemistry. *ChemPhysChem* **2020,** *21* (21), 2402.
55. Wijnen, J. W.; Engberts, J. B., Retro-Diels− Alder reaction in aqueous solution: toward a better understanding of organic reactivity in water. *The Journal of organic chemistry* **1997,** *62* (7), 2039-2044.
56. van Der Wel, G. K.; Wijnen, J. W.; Engberts, J. B., Solvent Effects on a Diels− Alder Reaction Involving a Cationic Diene: Consequences of the Absence of Hydrogen-Bond Interactions for Accelerations in Aqueous Media. *The Journal of organic chemistry* **1996,** *61* (25), 9001-9005.
57. Stevenson, R.; De Bo, G., Controlling reactivity by geometry in retro-diels–alder reactions under tension. *Journal of the American Chemical Society* **2017,** *139* (46), 16768-16771.
58. Su, X.; Chen, B., Tough, resilient and pH-sensitive interpenetrating polyacrylamide/alginate/montmorillonite nanocomposite hydrogels. *Carbohydr Polym* **2018,** *197*, 497-507.

59. Zhuang, Y.; Yu, F.; Chen, H.; Zheng, J.; Ma, J.; Chen, J., Alginate/graphene double-network nanocomposite hydrogel beads with low-swelling, enhanced mechanical properties, and enhanced adsorption capacity. *Journal of Materials Chemistry A* **2016,** *4* (28), 10885-10892.
60. Novikov, V.; Kuzmin, V.; Kuznetsov, S.; Darvin, M.; Lademann, J.; Sagitova, E.; Ustynyuk, L. Y.; Prokhorov, K.; Nikolaeva, G. Y., DFT study of Raman spectra of polyenes and ß-carotene: Dependence on length of polyene chain and isomer type. *Spectrochimica Acta Part A: Molecular and Biomolecular Spectroscopy* **2021,** *255*, 119668.
61. Sun, J.-Y.; Zhao, X.; Illeperuma, W. R.; Chaudhuri, O.; Oh, K. H.; Mooney, D. J.; Vlassak, J. J.; Suo, Z., Highly stretchable and tough hydrogels. *Nature* **2012,** *489* (7414), 133-136.
62. Buche, M. R.; Silberstein, M. N., Chain breaking in the statistical mechanical constitutive theory of polymer networks. *arXiv preprint arXiv:2104.08866* **2021**.
63. Larsen, M. B.; Boydston, A. J., Successive mechanochemical activation and small molecule release in an elastomeric material. *J Am Chem Soc* **2014,** *136* (4), 1276-9.
64. Li, N.-N.; Zhang, Y.-L.; Mao, S.; Gao, Y.-R.; Guo, D.-D.; Wang, Y.-Q., Palladium-catalyzed C–H homocoupling of furans and thiophenes using oxygen as the oxidant. *Organic letters* **2014,** *16* (10), 2732-2735.
65. Sivanantham, M.; Kesavamoorthy, R.; Sairam, T.; Sabharwal, K.; Raj, B., Stimulus response and molecular structural modification of polyacrylamide gel in nitric acid: A study by Raman, FTIR, and photoluminescence techniques. *Journal of Polymer Science Part B: Polymer Physics* **2008,** *46* (7), 710-720.
66. Levin, I. W.; Harris, W., Interpretation of the vibrational spectra of bicyclic hydrocarbons: norbornane and norbornadiene. *Spectrochimica Acta Part A: Molecular Spectroscopy* **1973,** *29* (10), 1815-1834.
67. Gupta, M. K.; Bansil, R., Laser Raman spectroscopy of polyacrylamide. *Journal of Polymer Science: Polymer Physics Edition* **1981,** *19* (2), 353-360.
68. HORIBA, Raman Spectroscopy for Analysis and Monitoring